Korean J. Chem. Eng., **28**(2), 608-612 (2011)
DOI: 10.1007/s11814-010-0396-z

Impact of electrolyte additives (alkali metal salts) on the capacitive behavior of NiO-based capacitors

Yong Zhang†, Lizhen Wang, Aiqin Zhang, Yanhua Song, Xiaofeng Li, Xingbing Wu, Peipei Du, and Lv Yan

Henan Provincial Key Laboratory of Surface & Interface Science,
Zhengzhou University of Light Industry, Zhengzhou 450002, China
(*Received 20 May 2010 • accepted 30 July 2010*)

Abstract−To improve the specific capacitance and energy density of electrochemical capacitor, nanostructured NiO was prepared by high temperature solid-state method as electrode material. The crystal structure and morphology of as-parepared NiO samples were investigated by X-ray diffraction (XRD) and scanning electron microscopy (SEM). Cyclic voltammetry (CV) measurement was applied to investigate the specific capacitance of the NiO electrode. Furthermore, a novel mixed electrolyte consisting of NaOH, KOH, LiOH and Li_2CO_3 was prepared for the NiO capacitor, and the component and concentration of the four different electrolytes was examined by orthogonal test. The results showed that the NiO sample has cubic structure with nano-size particles, and the optimal composition of the electrolyte was: NaOH 2 mol L^{-1}, KOH 3 mol L^{-1}, LiOH 0.05 mol L^{-1}, and Li_2CO_3 0.05 mol L^{-1}. At a scan rate of 10 mV s^{-1}, the fabricated capacitor exhibits excellent electrochemical capacitive performance, while the specific capacitance and the energy density were 239 F g^{-1} and 85 Wh kg^{-1}, which was higher than one-component electrolyte.

Key words: Mixed Electrolyte, Nickel Oxide, Orthogonal Test, Optimal Composition

INTRODUCTION

Electrochemical capacitors (ECs) have been attracting considerable attention due to their large specific capacitance and potential application in hybrid vehicles and memory back-up systems. However, compared with usual batteries, the lower energy density is the greatest drawback of the ECs. In recent years, extensive work has focused on ways to improve both the power and energy density of ECs [1-4]. The performance of ECs depends strongly on the component and concentration of electrolytes and the specific surface area of the electrode materials [5].

Because of the low utilization of the carbon-based material and degradation of the conducting polymer material, many researches aim to increase the power and energy density of ECS as well as lower fabrication costs while using environmental friendly materials [6-8]. The amorphous form of hydrous ruthenium oxides was found to be a promising material for high power and high energy density of ECs, but the cost problem restricts their widespread usages [9-11]. Up to now, NiO has become a promising candidate material for the ECs due to its inexpensive and excellent performance [12]. Especially for the nano-NiO, which plays a excellent electrochemical capacitive performance in ECs due to its high specific surface area and fast redox reactions [13].

Generally, the ECs electrolytes are classified into organic and aqueous solutions [14,15]. The organic ECs system is more effective in energy storage from the viewpoint of its wider potential window compared with that of an aqueous, but the leakage or evaporation of the solvent from the organic electrolyte solutions limits its long-term stability [16]. In the case of aqueous system, the fabrication processes of the ECs are easy. However, most of the aqueous system is one-component electrolyte [17,18]. To increase the performance of ECs, we used the mixed electrolyte in this experiment.

In this paper, in order to improve the performances of ECs, nano-NiO was prepared by high temperature solid-state method. Furthermore, we applied the mixed electrolyte consisting of NaOH, KOH, LiOH, and Li_2CO_3 to NiO ECs, and the component and concentration of the four different electrolytes was studied by orthogonal test. At a scan rate of 10 mV s^{-1}, the fabricated capacitor exhibits excellent electrochemical capacitive performance, while the specific capacitance and the energy density were 239 F g^{-1} and 85 Wh kg^{-1}, which was higher than one-component electrolyte. To our knowledge, using the orthogonal experiment to study the optimum condition of the mixed electrolyte has not been reported.

EXPERIMENTAL

1. Synthesis of the NiO

The nano-NiO was prepared by high temperature solid-state method. The precursor was prepared by grinding oxalic acid with nickel acetate tetrahydrate for 30 min (the molar ratio was 1 : 1), and the reseda powder was obtained, then the powders were calcined at 350 °C for 2 hours to obtain the final product NiO. The as-prepared NiO was characterized X-ray diffraction (XRD, Bruker D8) and scanning electron microscopy (SEM, JSM-2100).

2. Electrochemical Tests

The cathode electrode was formed by mixing 87 wt% NiO, 10 wt% Super P (SP) and 3 wt% polytetrafluoroethylene (PTFE) as binder, and then was pressed onto nickel foam which serves as a current collector. The anode electrode was prepared by mixing 80 wt% active carbon, 10 wt% SP and 10 wt% PTFE. The measurements of cyclic voltammetry (CV) were performed in a three-elec-

†To whom correspondence should be addressed.
E-mail: zy@zzuli.edu.cn

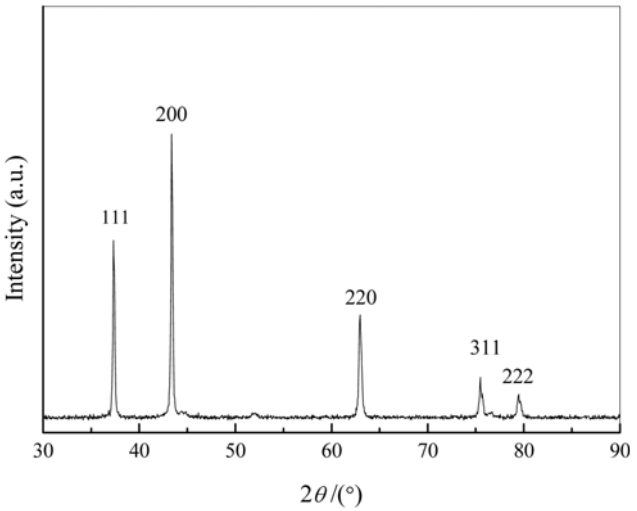

Fig. 1. XRD patterns of synthesized NiO powder.

trode cell at a scan rate of 10 mV s^{-1}. The cathode electrode, anode electrode and Hg/HgO electrode were used as the working, counter and reference electrodes, respectively. A CHI660B electrochemical workstation was employed for obtaining the electrochemical impedance spectra (EIS) with the frequency range from 100 KHz to 0.01 Hz at a voltage amplitude of 5 mV.

RESULTS AND DISCUSSION

1. XRD

Fig. 1 shows the XRD pattern of NiO powder prepared by high temperature solid-state method. The diffraction peaks at 37.2°, 43.3°, 62.9°, 75.4° and 79.4° are the typical character diffraction peaks of NiO, which agrees with that of the standard values [19]. All these diffraction peaks, including not only the peak positions but also their relative intensities, can be perfectly indexed into the cubic crystalline structure of NiO (JCPDS card 65-5745, a=4.177 nm, b=4.177 nm, c=4.177 nm). The grain size of the NiO crystalline is calculated from the major diffraction peak (200) using Scherrer's formula [18] (Eq. (1)):

$$D=0.89\lambda/B\cos\theta \quad (1)$$

Where D is the average crystallite size; λ is the wavelength used; B is the full width at half maximum of the peak, θ is Bragg's angle of the XRD peak. The grain size was found to be about 34.6 nm.

2. SEM

Fig. 2 shows the SEM images of the as-prepared NiO powders at different magnifications. From the observed SEM images, it can be seen that the powders consist of agglomerates with different shapes (Fig. 2(a)). The agglomerates themselves consist of very fine particles (Fig. 2(b) and Fig. 2(c)) with sizes under 80 nm. The nanostructure of NiO was thought to be beneficial to ionic charge transport and enhancing the capacitance due to surface effects.

3. Orthogonal Test Results and Discussions

It is well known that the electrolyte composition has an important effect on the performance of the capacitor. Therefore, the mixed electrolyte with NaOH, KOH, LiOH and LI_2CO_3 was studied to increase the electrochemical capacitive performance of NiO capacitor. The best performance would be exerted when the composition of the mixed electrolyte was optimized. Hence, the quantity of the above four factors was examined in the following ranges: quantity of NaOH: 1-3 mol L^{-1}, quantity of KOH: 1-3 mol L^{-1}, quantity of LiOH: 0.050-0.100 mol L^{-1}, and quantity of Li_2CO_3: 0.050-0.100

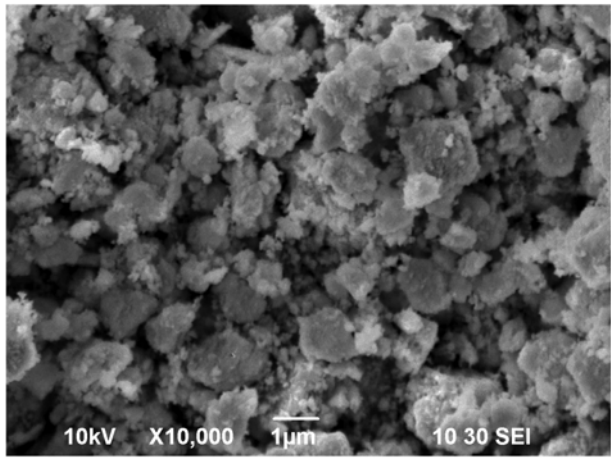

(a)

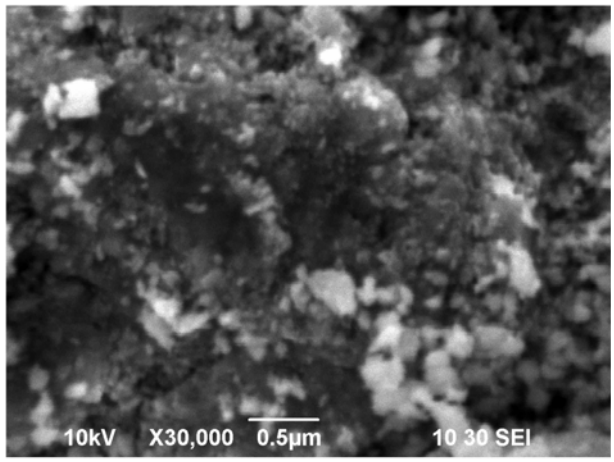

(b)

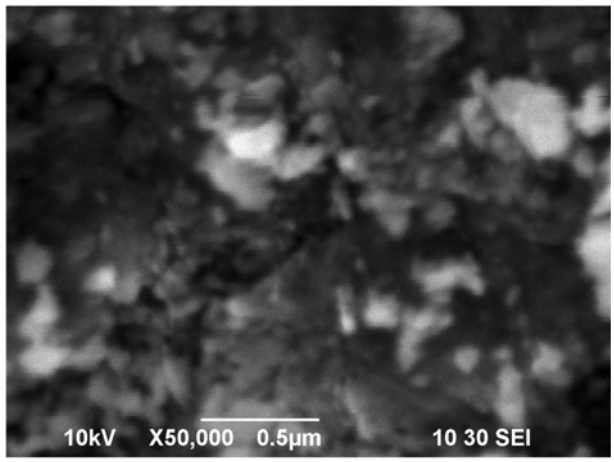

(c)

Fig. 2. SEM images of the as-prepared NiO powders at different magnifications: (a) 10,000×, (b) 30,000×, and (c) 50,000×.

Table 1. The orthogonal test factors and levels

Factors and levels	NaOH/ mol L^{-1}	KOH/ mol L^{-1}	LiOH/ mol L^{-1}	Li_2CO_3/ mol L^{-1}
1	1	1	0.050	0.050
2	2	2	0.075	0.075
3	3	3	0.100	0.100

Table 2. The orthogonal test results

	NaOH/ mol L^{-1}	KOH/ mol L^{-1}	LiOH/ mol L^{-1}	Li_2CO_3/ mol L^{-1}	Capacitance/ mol L^{-1}
1	1	1	0.050	0.050	100.80
2	1	2	0.075	0.075	46.51
3	1	3	0.100	0.100	59.78
4	2	1	0.075	0.100	52.01
5	2	2	0.100	0.050	116.86
6	2	3	0.050	0.075	219.84
7	3	1	0.100	0.075	88.50
8	3	2	0.050	0.100	62.55
9	3	3	0.075	0.050	169.38
I	69.03	80.44	127.73	129.01	
II	129.57	75.31	89.3	118.28	
III	106.81	149.67	88.38	58.11	
R_j	60.54	74.36	39.35	70.90	

mol L^{-1}. Three levels were then chosen in each test factor. The test project contains four factors-three levels (see Table 1) The results are shown in Table 2. The specific capacitance can be calculated from CVs according to Eq. (2).

3-1. Effect of Electrolyte Composition on the Specific Capacitance of NiO Capacitor

The effect of the mixed electrolyte composition on the specific capacitance of NiO capacitor is shown in Fig. 3. Fig. 3(a) shows the effect of NaOH density on the specific capacitance of NiO. It is obvious that the specific capacitance increases first, and then decreases with an increase of KOH density; the capacitance reaches the maximum value when the NaOH concentration is 2 mol L^{-1}. The reason may be due to the diameter of Na^+. The ion with small diameter can be easy to pass through the micropores of the electrode in a short time, so the resistance is small, leading to an increase of specific capacitance. However, the transmission speed becomes smaller when the NaOH density is large enough, which leads to a decrease of capacitance.

The relationship between the KOH density and specific capacitance is shown in Fig. 3(b). The results show that the specific capacitance first decreased then increased with the increasing of KOH density. The maximum value of capacitance was obtained when the concentration was 3 mol L^{-1}. The main reason was due to the increased double-layer capacitance after the addition of KOH, and the double-layer capacitance relates to the ion concentration. Within a certain range of concentration, the double-layer is compressed gradually with the increasing of KOH density, and the thickness of the layer is decreased, leading to the increase of double-layer capacitance. As shown in Fig. 3(c) and Fig. 3(d), the capacitance decreases

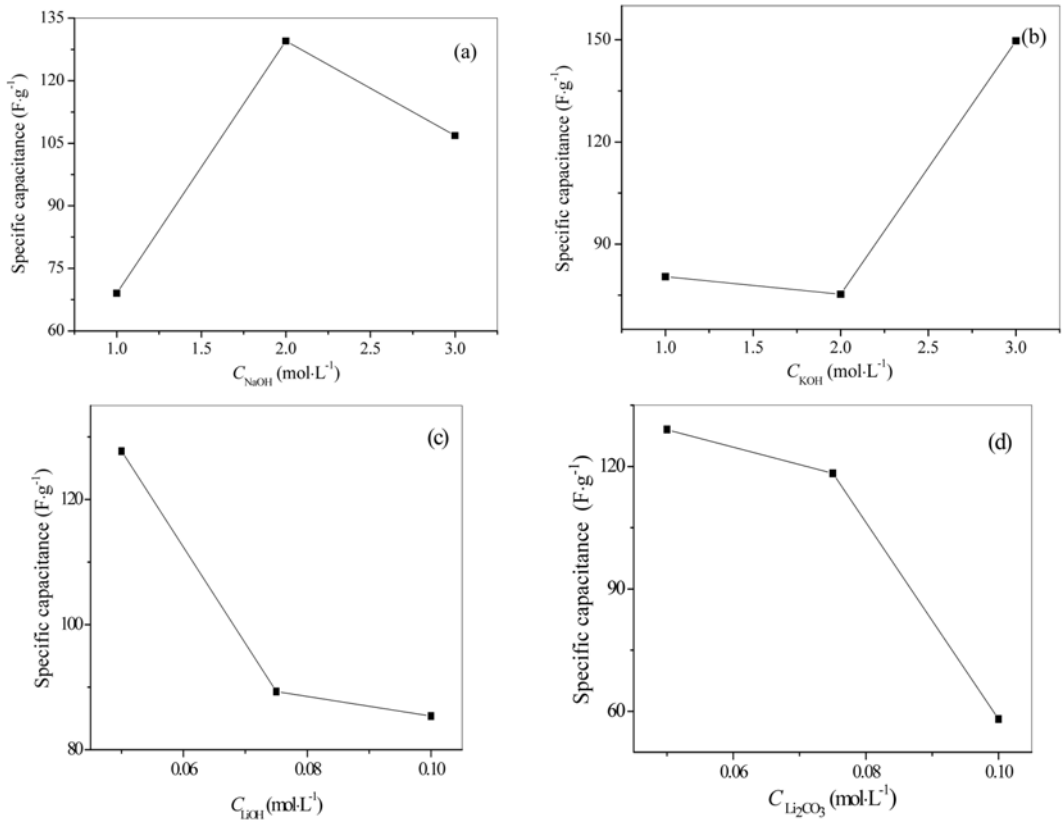

Fig. 3. Effects of four electrolyte compositions on the specific capacitance of NiO capacitor: (a) NaOH, (b) KOH, (c) LiOH, and (d) Li_2CO_3.

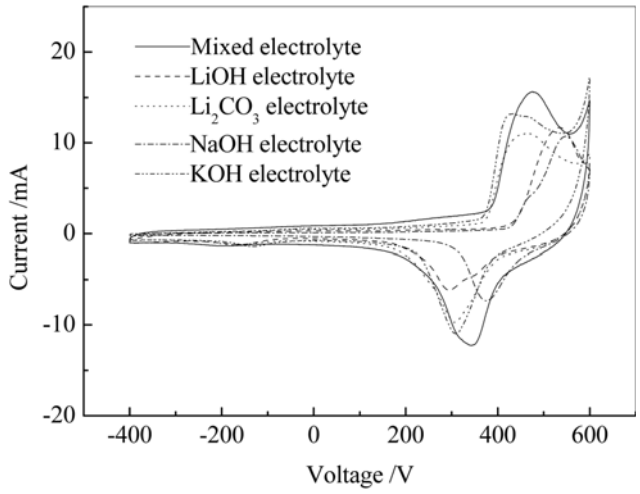

Fig. 4. CV curves of the NiO electrodes in different electrolytes at scan rate of 10 mV s^{-1}.

with an increase of LiOH and Li_2CO_3 density. It is demonstrated that the Li^+ has important effect on the performance of capacitor.

3-2. The Optimal Results

Key factors were ranked according to the maximum difference R_j (range values) of each column; their significance can be graded in order. The bigger the R_j is, the more significant the factor will be, and results are listed in Table 2. This enables the deduction that effects caused by different factor's level are different. The analysis results showed that the R_j values of the NaOH, KOH, LiOH, and Li_2CO_3 were 60.54, 74.36, 39.35, and 70.90, respectively. The effect of KOH on discharge specific capacitance was the most important and Li_2CO_3 was the second, followed by NaOH and LiOH, and the optimal composition of the mixed electrolyte was: NaOH 2 mol L^{-1}, KOH 3 mol L^{-1}, LiOH 0.05 mol L^{-1}, and Li_2CO_3 0.05 mol L^{-1}.

4. CV Results

CV curve was considered to be a suitable tool to characterize the capacitive behavior of electrode materials. Fig. 4 shows the CV curves of NiO electrodes in different electrolytes at scan rate of 10 mV s^{-1}. The CV curves show that the NiO electrodes in different electrolytes exhibited similar behavior; there is a pair of anodic and cathodic peaks centered at 0.32 and 0.45 V versus Hg/HgO, respectively. It is distinguished from that of the electric double-layer capacitance in which the shape of CV curves is usually close to an ideal rectangular shape, indicating that the capacity mainly results in the pseudocapacitance from the Ni^{3+}/Ni^{2+} reversible redox process. However, it also can be seen that the area under the current and potential curve involved during oxidation and reduction of NiO electrode in mixed electrolyte (2 mol L^{-1} NaOH+3 mol L^{-1} KOH+0.05 mol L^{-1} LiOH+ 0.05 mol L^{-1} Li_2CO_3) at scan rate of 10 mV s^{-1} appears to be the biggest among the five electrolytes, which means that the capacitance characteristic of the mixed electrolyte was superior to one-component electrolyte. The specific capacitance (C_m) can be calculated form CV curves according to Eq. (2).

$$C_m = \frac{1}{2\Delta V m \nu_0}\int_{V_{initial}}^{V_{final}} |i| dV \quad (2)$$

Where C_m is the specific capacitance of active material, ΔV is voltage difference, ν_0 is the scan rate, $V_{initial}$ is initial voltage, V_{final} is the final voltage, and the m is the amount of active material. The calculation results showed that the specific capacitance of NiO tested in mixed electrolyte, KOH, Li_2CO_3, NaOH, and LiOH was 239, 186, 146, 137, and 130 F g^{-1}, respectively.

The energy density (E) was obtained from Eq. (3).

$$E = \frac{1}{2} C_m V^2 \quad (3)$$

Where C_m is the specific capacitance and (V) is the voltage. The calculation results showed that the energy density of the mixed electrolyte, KOH, Li_2CO_3, NaOH, and LiOH was 85, 66, 52, 49, and 46 Wh kg^{-1}, respectively.

The as-prepared sample shows an excellent capacitance performance in the mixed electrolyte. For the mixed electrolyte, the least ionic transfer and diffusion resistance led to an excellent capacitance retention property. For one-component electrolyte, due to the larger solvated ion diameter and higher ion transfer resistance, the capacitive performance was inferior to the mixed electrolyte in terms of specific capacitance and power density.

5. EIS Results

EIS, as a powerful technique for the investigation of capacitive behavior of electrochemical cells, has also been used to check the ability of NiO electrodes to store electrical energy. Fig. 5 shows the Nyquist plots of NiO electrodes in the mixed electrolyte, KOH, $LiCO_3$, NaOH, and LiOH aqueous electrolyte. The Nyquist plots exhibit arc shape in high frequency range and an inclined straight line in low frequencies. From the point intersecting with the real axis in the range of high frequency, it can be seen that the values of the internal resistance of electrolyte were estimated as little as ca. 0.40 Ω for the mixed electrolyte under this experimental condition [17], and the electrolyte resistances of KOH, $LiCO_3$, NaOH and LiOH were 0.41, 0.42, 0.43 and 0.44 Ω, respectively. It is demonstrated that the mixed electrolyte has high ionic conductivity compared with one-component electrolyte. On the other hand, a line close to 90° attributed to a capacitive behavior was observed for the mixed electro-

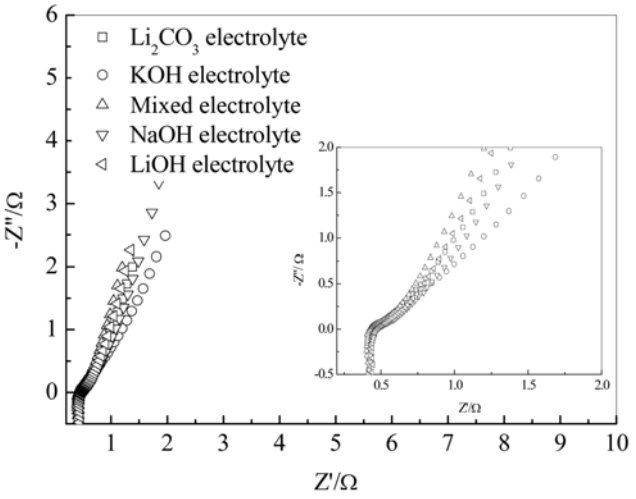

Fig. 5. Nyquist plots of the NiO electrodes in different electrolytes between 0.01 Hz and 100 KHz. Inset shows a magnified area of the plot for the high frequency range.

lyte, which means that the mixed-based capacitor may contain the pseudocapacitance of a few percent of total capacitance [20]. Therefore, the pseudocapacitance may be responsible for the high capacitance for the mixed electrolyte than that for the KOH, $LiCO_3$, NaOH or LiOH aqueous solution, which agrees well with the CV results.

CONCLUSIONS

The nano-NiO was prepared by high temperature solid-state method for the electrode material of ECs. The XRD results showed that the NiO was cubic crystalline structure, and the grain size of the crystalline was 34.6 nm. On the other hand, in order to enhance the specific capacitance and energy density of ECs, we have applied a mixed electrolyte consisting of NaOH, KOH, LiOH and Li_2CO_3 to NiO capacitor, and the component and concentration of the five different electrolytes was examined by orthogonal test. The effect of KOH on discharge specific capacitance was the most important and Li_2CO_3 was the second, followed by NaOH and LiOH, and the optimal composition of the mixed electrolyte was: NaOH 2 mol L^{-1}, KOH 3 mol L^{-1}, LiOH 0.05 mol L^{-1}, and Li_2CO_3 0.05 mol L^{-1}. At a scan rate of 10 mV s^{-1}, the fabricated capacitor exhibits excellent electrochemical capacitive performance, while the specific capacitance and the energy density were 239.0 F g^{-1} and 85 Wh kg^{-1}, which was higher than one-component electrolyte.

ACKNOWLEDGEMENTS

This work was supported by the National Natural Science Foundation of China (Project No. 21001097), the Basic and Frontier Technology Research Program of Henan Province, China (Project No. 102300410107), the Project for Outstanding Young Teachers in Higher Education Institutions of Henan Province (Project No. Henan Higher Education [2009]844), the Key Projects of Science and Technology in Zhengzhou City (Project No. 0910SGYG23259), and the Key Projects of Science and Technology in Jinshui District, Zhengzhou City (Project No. [2009]35-35).

REFERENCES

1. Y. Zhang, H. Feng, X. Wu, L. Wang, A. Zhang, T. Xia, H. Dong, X. Li and L. Zhang, *Int. J. Hydrogen Energy*, **34**, 4889 (2009).
2. S. Yamazaki, K. Obata, Y. Okuhama, Y. Matsuda, M. Yamagata and M. Ishikawa, *J. Power Sources*, **195**, 1753 (2010).
3. M. Selvakumar and S. Pitchumani, *Korean J. Chem. Eng.*, **27**, 977 (2010).
4. S. W. Lee, D. K. Park, J. K. Lee, J. B. Ju and T. W. Sohn, *Korean J. Chem. Eng.*, **18**, 371 (2001).
5. H. Wang and M. Yoshio, *J. Power Sources*, **195**, 1263 (2010).
6. C.-C. Yang and G. M. Wu, *Mater. Chem. Phys.*, **114**, 948 (2009).
7. R. K. Sharma and L. Zhai, *Electrochim. Acta*, **54**, 7148 (2009).
8. Y. Liu, W. Zhao and X. Zhang, *Electrochim. Acta*, **53**, 3296 (2008).
9. S. R. Sivakkumar, J. M. Ko, D. Y. Kim, B. C. Kim and G. G. Wallace, *Electrochim. Acta*, **52**, 7377 (2007).
10. E. C. Rios, A. V. Rosario, R. M. Q. Mello and L. Micaroni, *J. Power Sources*, **163**, 1137 (2007).
11. F. Pico, J. Ibañez, T. A. Centeno, C. Pecharroman, R. M. Rojas, J. M. Amarilla and J. M. Rojo, *Electrochim. Acta*, **51**, 4693 (2006).
12. M.-S. Wu and H.-H. Hsieh, *Electrochim. Acta*, **53**, 3427 (2008).
13. M.-S. Wu, Y.-A. Huang, C.-H. Yang and J.-J. Jow, *Int. J. Hydrogen Energy*, **32**, 4153 (2007).
14. G.-H. Sun, K.-X. Li and C.-G. Sun, *J. Power Sources*, **162**, 1444 (2006).
15. A. Laheäär, H. Kurig, A. Jänes and E. Lust, *Electrochim. Acta*, **54**, 4587 (2009).
16. C.-P. Tien, W.-J. Liang, P.-L. Kuo and H.-S. Teng, *Electrochim. Acta*, **53**, 4505 (2008).
17. M.-S. Wu, C.-Y. Huang and K.-H. Lin, *J. Power Sources*, **186**, 557 (2009).
18. F.-B. Zhang, Y.-K. Zhou and H.-L. Li, *Mater. Chem. Phys.*, **83**, 260 (2004).
19. Y.-G. Wang and Y.-Y. Xia, *Electrochim. Acta*, **51**, 3223 (2006).
20. S. Nohara, H. Wada, N. Furukawa, H. Inoue, M. Morita and C. Iwakura, *Electrochim. Acta*, **48**, 749 (2003).